Geometric magnetic frustration in the *R*-type ferrite $SrSn_2Ga_{1.3}Cr_{2.7}O_{11}$ and the spinel-based chromates

I. D. Posen,[1] T. M. McQueen,[1] A. J. Williams,[1] D. V. West,[1] Q. Huang,[2] and R. J. Cava[1]
[1]*Department of Chemistry, Princeton University, Princeton, New Jersey 08544, USA*
[2]*Center for Neutron Research, NIST, Gaithersburg, Maryland 20899, USA*
(Received 18 December 2009; revised manuscript received 10 March 2010; published 8 April 2010)

$SrSn_2Ga_{1.3}Cr_{2.7}O_{11}$ is shown to be a strongly geometrically frustrated magnet through measurement of its temperature-dependent magnetic susceptibility and specific heat. This material, determined by powder neutron diffraction to have an *R*-type ferrite crystal structure, has $S=3/2$ Cr^{3+} ions in isolated Kagomé planes with no magnetic ions in the intermediary structural layers. The Kagomé planes contain 10% nonmagnetic Ga^{3+}. This structure type makes the chromate family of frustrated magnets unusual because it displays four spinel-based structural variants with the same basic magnetic lattice and different effective dimensionalities and degrees of frustration. A comparison of the structures and magnetic characteristics is presented.

DOI: 10.1103/PhysRevB.81.134413 PACS number(s): 75.50.Ee, 61.66.Fn, 75.47.Lx

I. INTRODUCTION

Geometric frustration of magnetic ordering occurs when it is unfavorable for the magnetic moments in a solid to order periodically over long distances due to competing interactions that are a consequence of the geometry of the lattice. Many compounds are known to display magnetic frustration at least to some degree (see, e.g., Refs. 1–9). Most often studied are the rare-earth pyrochlores, because their magnetic lattice of corner-sharing tetrahedra can be occupied by all of the rare earths, allowing for the study of different spin configurations and interactions within a single magnetic lattice geometry. Substantial changes in the geometry of the magnetic lattice in the pyrochlores are difficult to attain, however.[10] In contrast, one of the reasons for interest in frustrated chromates derived from the spinel structure is that the Kagomé-based magnetic lattice geometry can be varied for a single isotropic Heisenberg spin ion, Cr^{3+} ($S=3/2$). The previously known compounds in this family are the spinel $ZnCr_2O_4$ (e.g., Refs. 11–13) and the related phases $SrGa_4Cr_8O_{19}$—"SCGO" (e.g., Refs. 1, 14, and 15) an *M*-type ferrite, and $BaSn_2Ga_3ZnCr_7O_{22}$ (e.g., Refs. 16–18), a QS-ferrite. Here we report the characterization of $SrSn_2Ga_{1.3}Cr_{2.7}O_{11}$, a material which, as an *R*-type ferrite, expands the family of frustrated chromates to include substantially different degrees of effective magnetic dimensionality. The magnetic Kagomé planes in $SrSn_2Ga_{1.3}Cr_{2.7}O_{11}$ are widely separated and more magnetically isolated than for other Cr-based frustrated magnets. Comparison of the properties shows this to be one of the more extreme cases of magnetic frustration in the family.

II. EXPERIMENT

The design of this material was based on the *R*-type iron ferrite $BaFe_{4-2x}Sn_{2+x}Co_xO_{11}$.[19] Setting $x=0$ and replacing the four Fe^{3+} atoms by a 3:1 ratio of Cr^{3+} to nonmagnetic atoms, the goal was to find an *R*-type ferrite with the formula $ASn_2MCr_3O_{11}$, with Cr^{3+} on the Kagomé planes and intermediate planes with no magnetic ions present. Such a compound was indeed found. As observed for SCGO and the QS ferrite, however, pure Cr Kagomé layers without disorder are not achievable and the formula of the compound is $SrSn_2Ga_{1.3}Cr_{2.7}O_{11}$. Writing the formula alternatively as $SrSn_2Ga(Cr_{1-x}Ga_x)_3O_{11}$ with $x=0.1$ describes explicitly the 90% filling of the Kagomé planes with Cr and the $SrSn_2Ga$-oxide composition of the intermediary layers. Due to the thermodynamic stability of competing phases, unconventional conditions were needed for synthesis.[20] For comparison of the magnetic properties for all members of the family, polycrystalline samples of $ZnCr_2O_4$, $SrGa_4Cr_8O_{19}$, and $Ba_2Sn_2ZnGa_3Cr_7O_{22}$ were synthesized by conventional methods.[21] The purity of the samples was characterized by laboratory x-ray diffraction (Bruker D8 Focus, Cu $K\alpha$ radiation). The crystal structure of this material was determined by neutron powder diffraction (NPD) analysis with data collected at the NIST center for neutron research on the BT1 diffractometer. The NPD patterns at 298 K were obtained using a Cu (311) monochromator with a 90° takeoff angle, $\lambda=1.5404(2)$ Å and in-pile and diffracted beam collimations of 15′ and 20′, respectively. Data were collected over the two theta range 3°–168° with a step size of 0.05°. The GSAS program suite was used for Rietveld structural refinement.[22] Scattering lengths (in femtometer) employed in the refinement were 7.02, 6.23, 7.29, 3.63, and 5.80 for Sr, Sn, Ga, Cr, and O, respectively.

A Quantum Design physical properties measurement system (PPMS) instrument was employed for specific-heat and magnetization measurements. Magnetization (M) vs applied field (H) curves for all materials showed that M is linearly dependent on $\mu_0 H$ at least up to 0.5 T for all temperatures between 1.8 and 300 K, and therefore the temperature-dependent susceptibility, $\chi=M/H$, measurements were performed for all materials in a field of $\mu_0 H=0.2$ T. Specific-heat measurements were performed on $SrSn_2Ga_{1.3}Cr_{2.7}O_{11}$ in the PPMS for temperatures between 0.4 and 30 K. We adopt the ratio $f=|\theta|/T_N$ or $|\theta|/T_{SG}$, where θ is the Curie-Weiss θ and T_N and T_{SG} are the Néel or spin-glass ordering temperature, respectively, as a measure of the degree of magnetic frustration, f.[1] For the *M*-type and QS-type Cr-based ferrites, no T_N is observed and disorder on the Cr lattice leads to glassy behavior in the susceptibility; T_{SG} is used in those

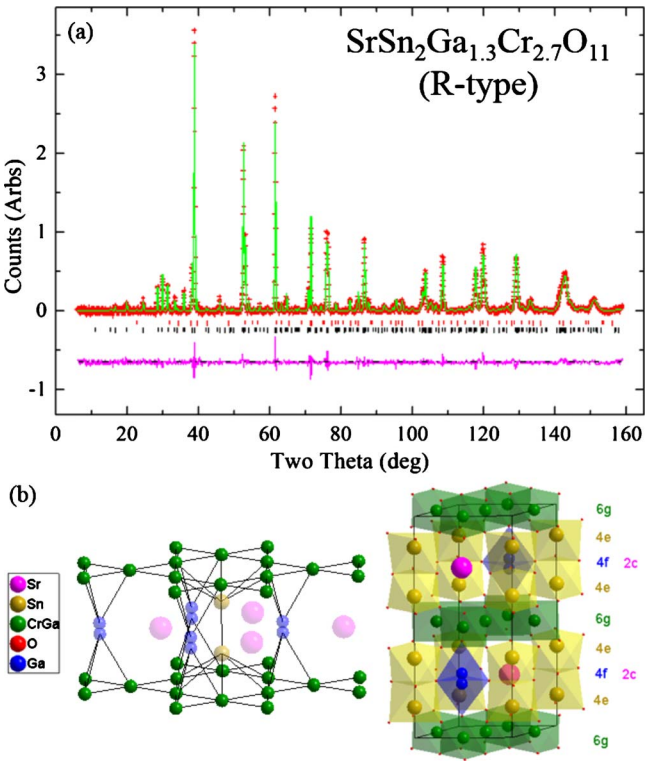

FIG. 1. (Color online) (a) Neutron powder-diffraction data, with Rietveld fits, of the *R*-type ferrite at 298 K. The tick marks correspond (from top to bottom) to (1%) $SrCr_2O_4$, (3%) Cr_2O_3, and the main phase, $SrSn_2Ga_{1.3}Cr_{2.7}O_{11}$, respectively. (b) The structure of $SrSn_2Ga_{1.3}Cr_{2.7}O_{11}$, emphasizing the oxygen coordination polyhedra of the metal atoms and the Kagomé planes.

cases. The condition $f>10$ is often used as a standard for a strongly frustrated system.[1]

III. RESULTS AND DISCUSSION

The results of the structure determination are shown in Fig. 1 and Table I. NPD data confirmed the crystal structure of $SrSn_2Ga_{1.3}Cr_{2.7}O_{11}$ to be the *R*-type ferrite type, space group $P6_3/mmc$. The nonmagnetic Sr ions are ordered into the large atom site (2*c* site) between the Kagomé planes, as expected for ferrites. Similarly, the nonmagnetic Sn ions fully occupy the large octahedrally coordinated sites (4*e* site) between the Kagomé planes, with no observed intermixing of other ions. The location of the nonmagnetic Ga ions within the triangular bipyramidal site between the Kagomé planes is split into two equivalent half occupied slightly off-center positions (4*f* site) as is commonly seen in ferrites, indicating that the relatively small Ga^{3+} ions prefer tetrahedral rather than fivefold coordination with oxygen. Free refinement of the occupancy of this site, testing whether it is partially occupied by Cr, revealed that no Cr is present, as is expected since this site has a highly unfavorable geometry for the Cr^{3+} ion. All Cr was found in the Kagomé layers. Free refinement of the Cr/Ga occupancies in the metal-oxygen octahedra that make up the Kagomé layers (6*g* site) shows that there is some mixture of Cr and Ga on this site. The refinement indicates a formula of $SrSn_2Ga_{1.3}Cr_{2.7}O_{11}$. The results indicate that the magnetic Cr atoms are perfectly confined to the Kagomé layer but that the Kagomé layer is diluted to 10% with nonmagnetic Ga ions. The formula of this ferrite can alternately be written as $SrSn_2Ga(Cr_{1-x}Ga_x)_3O_{11}$, with $x=0.10$, where x is the fraction of Kagomé plane sites filled with nonmagnetic Ga.

The temperature-dependent magnetic susceptibility χ of $SrSn_2Ga_{1.3}Cr_{2.7}O_{11}$ is shown in Fig. 2, as are the comparably collected magnetic susceptibilities of the other members of the spinel-derived chromate family. The main panel shows the data plotted as $1/(\chi+\chi_0)$ vs T, where χ is the measured susceptibility, M/H at an applied field of 0.2 T (where M vs H is linear for all materials), and χ_0 is a very small temperature independent background contribution. The fitted values of χ_0 are -7.1×10^{-5}, $+1.5\times10^{-4}$, -3.5×10^{-4}, and -1.3×10^{-4} emu/mol Cr, for the spinel, *M*, QS, and *R*-type ferrite samples, respectively, comparable to the values expected for core diamagnetism except for the *M*-type ferrite for which a small magnetic contribution, about 1% of the total susceptibility at 2 K, is present, likely due to a small amount of impurity phase. Curie-Weiss fitting to the data in the range 250–300 K (200–300 K fits yield similar results) yields values for θ and the effective magnetic moment per Cr, (see Table II). As is often the case in strongly frustrated magnets, Curie-Weiss fitting can only be viewed as approximate because these compounds all show very large values of θ, re-

TABLE I. Refined structural parameters for $SrSn_2Ga_{1.3}Cr_{2.7}O_{11}$ at room temperature. Space group $P6_3/mmc$, $z=2$, cell parameters: $a=5.8755(2)$ and $c=13.4982(5)$ Å. The sample contains 3% Cr_2O_3 and 1% $SrCr_2O_4$. The thermal parameters are in units of 10^{-2} Å^2.

Atom	Site	Occupancy	x	y	z	U_{iso}
Sr	2*c*	1	1/3	2/3	$\frac{1}{4}$	0.91(12)
Sn	4*e*	1	0	0	0.1387(3)	0.64(7)
Ga1	4*f*	0.5	1/3	2/3	0.7266(4)	0.60(13)
Cr	6*g*	0.91(2)	1/2	0	0	0.29(11)
Ga2	6*g*	0.09(2)	1/2	0	0	0.29(11)
O1	12*k*	1	0.1777(3)	0.3555(6)	0.0815(2)	0.78(5)
O2	6*h*	1	0.8477(4)	0.6953(8)	$\frac{1}{4}$	0.99(8)
O3	4*f*	1	1/3	2/3	0.5781(4)	0.66(10)

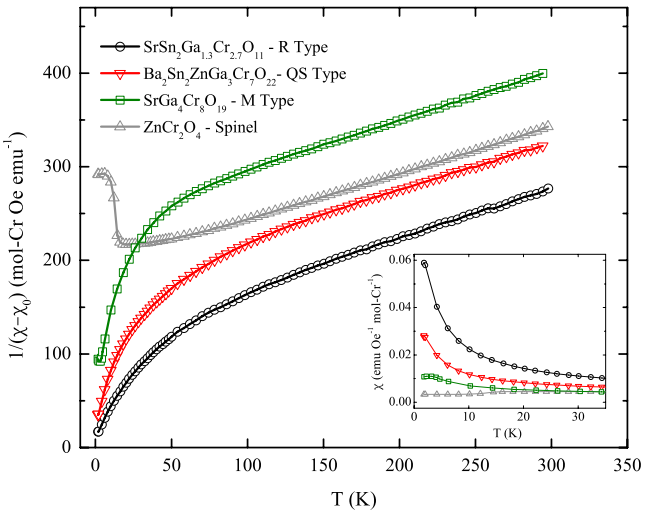

FIG. 2. (Color online) The variation in $1/(\chi-\chi_o)$ with temperature, measured in an applied field of at $\mu_0 H=0.2$ T, for the entire family of Cr-based ferrites. Inset: magnetic susceptibility versus temperature.

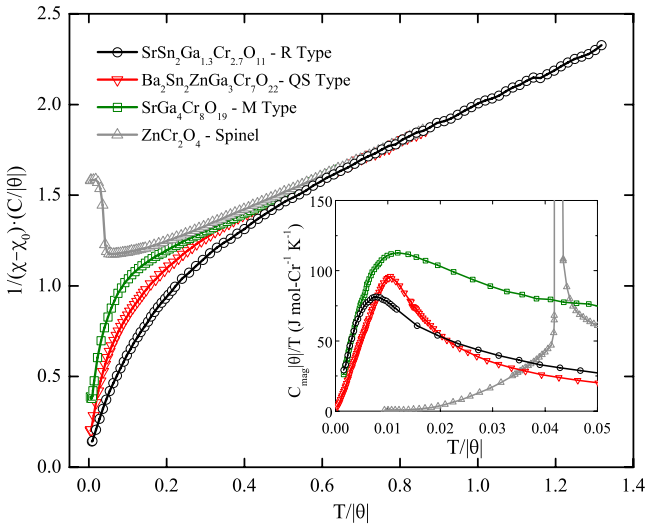

FIG. 3. (Color online) Main panel: normalized inverse susceptibility plots for the all members of the chromium ferrite family. Inset: normalized low-temperature specific heat of all members of the Cr-ferrite family. The specific-heat data for the spinel, *M*-type, and QS-type ferrites are taken from Ref. 16.

sulting in a fit of the susceptibility data well below θ in some cases; the fitting therefore yields somewhat different values for μ_{eff} and θ in different studies (i.e., compare the present results to those in Ref. 16) depending on the temperature range of the fits. For $SrSn_2Ga_{1.3}Cr_{2.7}O_{11}$, fitting the high-temperature data to the Curie-Weiss law, we find an effective magnetic moment per Cr^{3+} of $\mu_{\text{eff}}=3.9\mu_B$, which is near the ideal spin only value of 3.87 and comparable to what is typically observed for Cr^{3+}.[23] The fit further shows a value of $\theta=-226$ K, indicating strong antiferromagnetic coupling between spins. Using θ as a measure of the strength of the near neighbor magnetic interactions, we see that these are substantially weaker for the *R*-type ferrite than for the other compounds in the family. The susceptibility of $SrSn_2Ga_{1.3}Cr_{2.7}O_{11}$ starts to show significant deviations from Curie-Weiss behavior at temperatures as high as 100 K. The curling down of the $1/(\chi+\chi_0)$ plot is equivalent to an increase in χ, which indicates the presence of increasing ferromagnetic fluctuations on decreasing temperature. Failure of the compound to show sharp ordering features or differences between field-cooled and zero-field-cooled susceptibilities by 1.8 K indicates that any magnetic ordering or spin freezing occurs at lower temperatures and therefore a high degree of magnetic frustration; f is greater than $226/1.8 \approx 126$.

Comparison of the magnetic properties of all the members of the frustrated Kagomé chromates is of significant interest. To best compare the magnetic behavior for all members of the family, the Curie-Weiss law may be rewritten as $\frac{C}{|\theta|(\chi-\chi_0)}=\frac{T}{|\theta|}+1$ for $\theta<0$. This allows us to normalize the inverse susceptibility plots in terms of C and θ, which are obtained from the high-temperature fits. The resulting plot is presented in Fig. 3. At high temperatures, all data are concurrent as expected from the Curie-Weiss law. The most obvious observation from the normalized plot is that the hexagonal ferrites all show similar, significant ferromagnetic deviations from the Curie-Weiss law, at relatively high values of normalized temperature, $T/|\theta|$, whereas the spinel shows only minor antiferromagnetic deviations and only does so closer to its ordering temperature. A second feature of the normalized plot is the systematic trend in the deviation among the hexagonal ferrites. The *M*-type ferrite has the highest value of θ, is the last to deviate from Curie-Weiss behavior, and shows the sharpest curvature at low $T/|\theta|$. Conversely, the *R* type has the lowest value of θ and is the first to deviate but shows the weakest curvature at low $T/|\theta|$. The trend in normalized temperature at which deviations set in can be rationalized by noting that those with stronger an-

TABLE II. Magnetic parameters for the Cr ferrites. Ordering temperatures for spinel, *M*-type, and QS-type ferrites taken from Ref. 16.

Compound	θ (K)	μ_{eeff}/Cr (μ_B)	Ordering	Curie-Weiss deviations at intermediate T
$ZnCr_2O_4$—spinel	−350	3.9	Antiferro; 18 K	Antiferro
$SrGa_4Cr_8O_{19}$—*M* type	−460	3.9	Spin glass; 2.6 K	Ferro
$Ba_2Sn_2ZnGa_3Cr_7O_{22}$—QS	−340	4.0	Spin glass; 1.5 K	Ferro
$SrSn_2Ga_{1.3}Cr_{2.7}O_{11}$—*R* type	−226	3.9	None yet observed. Estimated 1.2 K	Ferro

tiferromagnetic interactions are the last to deviate ferromagnetically from the Curie-Weiss law; the normalized temperatures of the deviations do not monotonically scale with the frustration index "*f*." Theoretical modeling that explicitly compares the expected magnetic properties of the four distinctly different magnetic lattices involved would be of great interest in understanding the behavior of the full Cr-ferrite family represented in Fig. 3.

The inset of Fig. 3 shows the normalized heat-capacity data for each compound. For the spinel, *M*-type, and QS ferrites, the specific-heat data are taken from Ref. 16. For the *R*-type ferrite, where no nonmagnetic analog is known, the estimated phonon contribution to the specific heat is assumed to obey T^3 behavior at low temperatures and has been subtracted using the term $C_{lattice}=2.61\times10^{-4}\frac{\mathrm{J}}{\mathrm{mol\ CrK}^4}T^3$. This yields a Debye temperature of 370 K, consistent with what is expected for an oxide of this type. The temperature has been normalized to the Curie-Weiss θ. So that the area under the curve remains a measure of the entropy loss in each case, the *y* axis is also scaled by θ. For the *R*-type ferrite, we estimate that 1/3 of the expected magnetic entropy for a spin 3/2 system is recovered up to $T/|\theta|=0.1$. There is a sharp spike for $ZnCr_2O_4$, reflecting the coupled first-order magnetic and structural phase transitions.[24] In contrast, the broad peak in the other three compounds is reminiscent of the short-range-order feature that typically precedes a spin-glass transition. The broad peak for the *R*-type ferrite occurs at a temperature of 1.8(2) K. If spin-glass ordering is in fact present for the *R*-type ferrite at low temperatures, then the transition temperature can be estimated as about 1.2 K from the position of the broad peak in the specific heat.[1] The behaviors of the specific heats below the broad peaks near $T/|\theta|=0.01$ are not what is expected for conventional spin glasses, as has been pointed out elsewhere;[1,16] the behaviors are similar in the three Cr ferrites, especially for the *M*-type and *R*-type compounds.

Comparison of the magnetic lattices of all the known Cr-based ferrites is shown in Fig. 4. The spinel structure consists of infinite layers of intersecting Kagomé lattices, resulting in three-dimensional magnetic interactions. Projecting the structure along the cubic body diagonal, the three-dimensional nature of the spinel magnetic lattice is represented by corner-sharing tetrahedra; an ordered array of alternating Kagomé and triangular planes. The more complex ferrites have hexagonal cells, with the Kagomé and triangular layers stacked in different fashions along the hexagonal *c* axis. *M*-type and QS-type ferrites are constructed by taking two layers of the spinel sandwich (the "S-block") as the base unit and connecting them in ways that do not transmit magnetic interactions in three dimensions as strongly as is found for the spinel. In the *M*-type ferrite, the triangular layer between Kagomé planes alternates successively with a layer in which the connection is established via atoms directly over the hexagonal holes in the Kagomé net (the "R-block"). In the QS ferrite, the S-block spinel sandwiches are separated by a large distance by layers (the "Q-block") that contain only nonmagnetic atoms; causing this structure to be even more two dimensional. The *R*-type ferrite, the structure of our material, combines both kinds of connection found in the *M*-type ferrite (the S-block and the R-block) within each

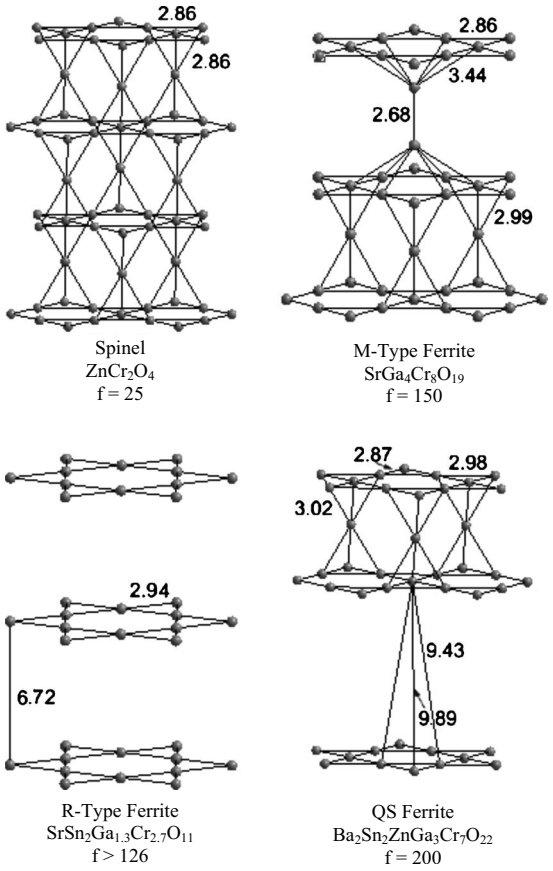

FIG. 4. A depiction of the magnetic sublattices for the spinel, *M*-type ferrite, QS ferrite, and *R*-type ferrite structures. Characteristic distances in angstroms are shown. *f* is the magnetic frustration ratio defined as θ/T_n or θ/T_{SG}; values of *f* for the spinel, *M*-type, and QS-type ferrites are taken from Ref. 16.

individual connecting layer. In this case, the magnetic lattice reduces to a system of isolated Kagomé planes, separated over large distances (6.7 Å) by nonmagnetic atoms. The resulting magnetic interactions are expected be almost perfectly two-dimensional because single Kagomé planes are involved, not the triple-layer sandwiches of Kagomé-triangle-Kagomé planes that are found in the other cases. In this context, it is surprising that the normalized magnetic behavior of $SrSn_2Ga_{1.3}Cr_{2.7}O_{11}$ is so similar to those of the *M*- and QS-type ferrites.

In conclusion, the *R*-type ferrite $SrSn_2Ga_{1.3}Cr_{2.7}O_{11}$, containing well-separated Kagomé planes of isotropic $S=3/2$ Cr^{3+} (but disordered with 10% nonmagnetic Ga^{3+}) was designed and then synthesized. Magnetic susceptibility and specific heat indicate strong antiferromagnetic interactions, $\theta=-226$ K, but no long range or spin-glass ordering down to 1.8 K, giving a frustration parameter of $f>126$. This compound is the fourth and most structurally two dimensional of the spinel-derived chromates; unlike the other members of the family, where magnetic Cr is found in triangular layers directly coupling nearby Kagomé planes, in the *R*-type ferrite the Kagomé planes are completely isolated from other Cr-containing planes. Normalized plots reveal striking similarities between the *M*-, QS-, and *R*-type ferrites; all show ferromagnetic deviations from Curie-Weiss behavior despite a

large antiferromagnetic Curie-Weiss θ. Future work is needed to understand why the ferrites behave in a magnetically similar fashion whether the magnetic system consists of a single Kagomé plane, as in the *R*-type ferrite, or two Kagomé planes coupled through an intermediary triangular plane as in the *M*-type and QS-type ferrites. It may be that the coupling between the Kagomé planes in the three layer sandwiches changes the behavior only quantitatively, not qualitatively. It may otherwise be that disorder in the Kagomé planes is the dominant factor in determining the observed behavior because those planes in all the Cr ferrites (with the exception of the spinel) contain a significant number of magnetic defects (10% in the *R*-type ferrite case). More detailed comparison of the impact of the disorder induced by nonmagnetic substitutions in the Kagomé planes in all the Cr ferrites may therefore be of future interest.

ACKNOWLEDGMENTS

This research was supported in part by the NSF program in solid-state chemistry, Grant No. NSF DMR-0703095. T.M.M. gratefully acknowledges the support by the National Science Foundation.

[1] A. P. Ramirez, Annu. Rev. Mater. Sci. **24**, 453 (1994).
[2] R. Moessner, Can. J. Phys. **79**, 1283 (2001).
[3] J. E. Greedan, J. Mater. Chem. **11**, 37 (2001).
[4] M. F. Collins and O. A. Petrenko, Can. J. Phys. **75**, 605 (1997).
[5] S. T. Bramwell and M. J. P. Gingras, Science **294**, 1495 (2001).
[6] P. Mendels, A. Olariu, F. Bert, D. Bono, L. Limot, G. Collin, B. Ueland, P. Schiffer, R. J. Cava, N. Blanchard, F. Duc, and J. C. Trombe, J. Phys.: Condens. Matter **19**, 145224 (2007).
[7] *Frustrated Spin Systems*, edited by H. T. Diep (World Scientific, Hackensack, NJ, 2004.
[8] S.-H. Lee, H. Takagi, D. Louca, M. Matsuda, S. Ji, H. Ueda, Y. Ueda, T. Katsufuji, J.-H. Chung, S. Park, S.-W. Cheong, and C. Broholm, J. Phys. Soc. Jpn. **79**, 011004 (2010).
[9] R. Moessner and J. T. Chalker, Phys. Rev. B **58**, 12049 (1998).
[10] G. C. Lau, R. S. Freitas, B. G. Ueland, B. D. Muegge, E. L. Duncan, P. Schiffer, and R. J. Cava, Nat. Phys. **2**, 249 (2006).
[11] D. Fiorani, J. Phys. C **17**, 4837 (1984).
[12] D. Fiorani, S. Viticoli, J. L. Dormann, J. L. Tholence, J. Hammann, A. P. Murani, and J. L. Soubeyroux, J. Phys. C **16**, 3175 (1983).
[13] H. Martinho, N. O. Moreno, J. A. Sanjurjo, C. Rettori, A. J. Garcı'a-Adeva, D. L. Huber, S. B. Oseroff, W. Ratcliff II, S.-W. Cheong, P. G. Pagliuso, J. L. Sarrao, and G. B. Martins, Phys. Rev. B **64**, 024408 (2001).
[14] X. Obradors, A. Labarta, A. Isalgue, J. Tejada, J. Rodriguez, and M. Pernet, Solid State Commun. **65**, 189 (1988).
[15] A. P. Ramirez, G. P. Espinosa, and A. S. Cooper, Phys. Rev. Lett. **64**, 2070 (1990).
[16] I. S. Hagemann, Q. Huang, X. P. A. Gao, A. P. Ramirez, and R. J. Cava, Phys. Rev. Lett. **86**, 894 (2001).
[17] H. Mutka, C. Payen, G. Ehlers, J. R. Stewart, D. Bono, and P. Mendels, J. Phys.: Condens. Matter **19**, 145254 (2007).
[18] D. Bono, P. Mendels, G. Collin, and N. Blanchard, Phys. Rev. Lett. **92**, 217202 (2004).
[19] B. Martínez, F. Sandiumenge, S. Gali, X. Obradors, and R. Rodriguez-Clemente, Solid State Commun. **83**, 649 (1992).
[20] SnO_2 (Aldrich 99.9%) and $SrCO_3$ (Alfa Aesar 99.99%) were ground and heated at 1000 °C in air for 2 days, reground, pressed into a pellet, and heated for a further 2 days under the same conditions in order to prepare $SrSnO_3$ as a starting material. Phase equilibria studies indicted that the *R*-type ferrite had a formula of the type $SrSn_2Ga_{1+x}Cr_{3-x}O_{11}$ with $0.2 \leq x \leq 0.3$. $SrSnO_3$, SnO_2, Ga_2O_3 (Aldrich 99.99%—predried at 550 °C in air for 2 h), and Cr_2O_3 (Fisher 99.85%) at a nominal $x=0.2$ were ground together with a 2% excess of $SrSnO_3$. The majority of the powder was pressed into a pellet and placed in a medium sized alumina crucible. The remaining loose powder was placed in a small alumina crucible, which was fitted inside the larger one. The resulting assembly was placed in a dry quartz tube, put under vacuum, heated mildly to remove surface water, backfilled with a small pressure of Ar, and sealed. Finally, the sealed tube was heated under N_2 at 1300 °C for 54 h. The pellet was extracted and sanded down to remove trace amounts of SiO_2 (from the quartz tube) and unreacted Cr_2O_3 from the surface. The pellet was then reground and reheated under the exact same procedure. For some samples, a third heating was required. The refined formula of the resulting phase, $SrSn_2Ga_{1.3}Cr_{2.7}O_{11}$, is slightly higher in Ga content than the nominal formula of $SrSn_2Ga_{1.2}Cr_{2.8}O_{11}$, consistent with our observation of the loss of some Cr during synthesis and very small amounts of Cr-containing impurities.
[21] $ZnCr_2O_4$ was prepared by grinding together stoichiometric amounts of ZnO (Alfa Aesar 99.9%) and Cr_2O_3 (Fisher 99.85%), pressing the powder into a pellet and heating in air at 1000 °C for 2 days. The product was reground, pressed to a pellet, and reheated in air at 1020 °C for a further 2 days. $SrGa_4Cr_8O_{19}$ was prepared by grinding together stoichiometric amounts of $SrCO_3$ (Alfa Aesar 99.99%), dry Ga_2O_3 (Aldrich 99.99%), and Cr_2O_3 (Fisher 99.85%). The sample was heated in air at 1000 °C for 48 h, 1200 °C for 24 h, and at 1350 °C for 36 h, with regrinding between each heating. $Ba_2Sn_2ZnGa_3Cr_7O_{22}$ was prepared by grinding together stoichiometric amounts of $BaCO_3$ (Alfa Aesar 99%), SnO_2 (Aldrich 99.9%), ZnO (Alfa Aesar 99.9%), dry Ga_2O_3 (Aldrich 99.99%), and Cr_2O_3 (Fisher 99.85%). The sample was heated in air at 1000 °C for 48 h, 1200 °C for 24 h, 1350 °C for 36 h, and again at 1350 °C for a further 19 h. The resulting powder was a phase-pure sample of $Ba_2Sn_2ZnGa_3Cr_7O_{22}$ confirming the reported formula (Ref. 16).
[22] A. Larson and R. B. Von Dreele, *GSAS: Generalized Structure Analysis System* (Los Alamos National Laboratory, Los Alamos, NM, 1994).
[23] H. P. Myers, *Introductory Solid State Physics* (Taylor & Francis, Bristol, 1997), p. 336.
[24] S. Ji, S.-H. Lee, C. Broholm, T. Y. Koo, W. Ratcliff, S.-W. Cheong, and P. Zschack, Phys. Rev. Lett. **103**, 037201 (2009).